

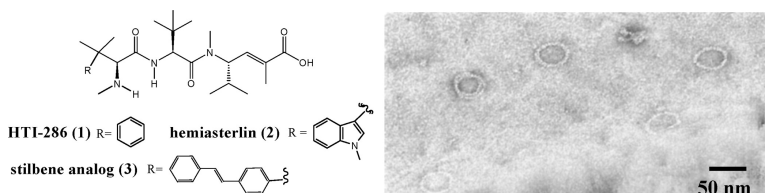
Communication

**Probing the Interaction of HTI-286 with Tubulin Using a Stilbene Analogue**

Mei-Chu Lo, Ann Aulabaugh, Girija Krishnamurthy, Joshua Kaplan, Arie Zask, Robert P. Smith, and George Ellestad

*J. Am. Chem. Soc.*, **2004**, 126 (32), 9898-9899 • DOI: 10.1021/ja048619e • Publication Date (Web): 21 July 2004

Downloaded from <http://pubs.acs.org> on April 1, 2009



**More About This Article**

Additional resources and features associated with this article are available within the HTML version:

- Supporting Information
- Access to high resolution figures
- Links to articles and content related to this article
- Copyright permission to reproduce figures and/or text from this article

[View the Full Text HTML](#)



**ACS Publications**  
 High quality. High impact.

## Probing the Interaction of HTI-286 with Tubulin Using a Stilbene Analogue

Mei-Chu Lo,<sup>\*,†</sup> Ann Aulabaugh,<sup>†</sup> Girija Krishnamurthy,<sup>†</sup> Joshua Kaplan,<sup>‡</sup> Arie Zask,<sup>‡</sup>  
Robert P. Smith,<sup>§</sup> and George Ellestad<sup>†</sup>

*Biophysics/Enzymology-Chemical and Screening Sciences, Medicinal Chemistry-Chemical and Screening Sciences, and Vaccines Research, Wyeth Research, 401 North Middletown Road, Pearl River, New York 10965*

Received March 10, 2004; E-mail: lom@wyeth.com

HTI-286 (**1**) (Figure 1) is a synthetic analogue of the natural product hemiasterlin (**2**), a potent antitubulin agent.<sup>1</sup> Hemiasterlins are tripeptides with three highly modified amino acids, which give rise to their *in vivo* stability and activity. The relative structural simplicity of hemiasterlins allows for diverse structural manipulation of the molecule via total synthesis. Among a series of hemiasterlin analogues synthesized at Wyeth and UBC,<sup>2</sup> HTI-286, containing a phenyl group instead of an indole as in hemiasterlin, is a potent inhibitor of cell proliferation and has substantially less interaction with the multidrug resistance protein (P-glycoprotein) than currently used antitumor agents.<sup>3</sup> In our previous report, we found that HTI-286 binds tubulin and induces the formation of a stable oligomer with 13 tubulin units.<sup>4</sup> The ability of HTI-286 to accommodate large substituents on the phenyl ring and still maintain the antitubulin potency<sup>2,5</sup> prompted us to synthesize a derivative (**3**) containing the chromophore stilbene (Figure 1) to further characterize this ligand-induced association.<sup>6</sup> The stilbene analogue has UV absorbance distinct from protein (Figure 2), which allows us to obtain the binding stoichiometry and to probe the binding site. Herein we describe our findings from analytical ultracentrifugation experiments using this stilbene analogue.

Analytical ultracentrifugation is a solution-based method used previously to study tubulin association induced by magnesium or antitubulin agents including vinca alkaloids and cryptophycin.<sup>7–9</sup> To investigate the effect of **3** on tubulin, we conducted sedimentation velocity experiments at different ratios of inhibitor to protein. Sedimentation was monitored alternately at wavelengths dominated by protein (262 nm, >90% of signal from protein) and by inhibitor (312 nm, signal from **3** alone). The sedimentation profiles were analyzed using SEDFIT<sup>10</sup> to generate the sedimentation coefficient distribution *c*(*s*) as shown in Figure 3.

In the absence of inhibitor (0  $\mu\text{M}$  in Figure 3), the monomeric tubulin (defined as an  $\alpha/\beta$  heterodimer, 100 kDa) migrates with a sedimentation coefficient of ca. 5.3 S. When more than 1 equiv of **3** (15.2  $\mu\text{M}$  in Figure 3) was added to 10  $\mu\text{M}$  tubulin, a major species with a sedimentation coefficient of ca. 17.4 S appears at 262 and 312 nm. This 17.4 S species is a stable ring (Figure 4). The outer diameter of the ring is 35–50 nm, similar to the dimension reported for the ring structure of tubulin induced by hemiasterlin.<sup>1</sup> The amounts of tubulin and **3** in the ring were estimated from the area under the 17.4 S peak detected at 262 and 312 nm, respectively. The analysis generates 10  $\mu\text{M}$  tubulin and 10  $\mu\text{M}$  of **3**, indicating that the binding stoichiometry in the ring is one inhibitor per tubulin monomer.

In the sample containing 1.9  $\mu\text{M}$  of **3** and 10  $\mu\text{M}$  tubulin, two peaks at 5.3 and 8.1 S appear at 262 nm, but only one peak at 8.1 S exists at 312 nm. It is likely that the 8.1 S species is tubulin

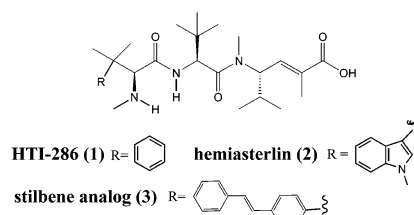


**Figure 1.** Chemical structures of HTI-286, hemiasterlin, and the stilbene analogue.

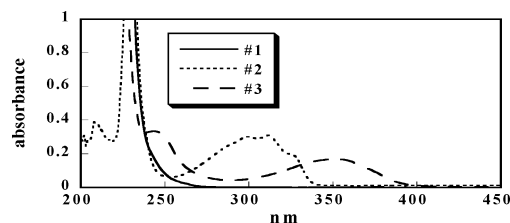


**Figure 2.** UV spectra of 50  $\mu\text{M}$  HTI-286 (curve 1), 10  $\mu\text{M}$  **3** (curve 2), and 10  $\mu\text{M}$  colchicine (curve 3).

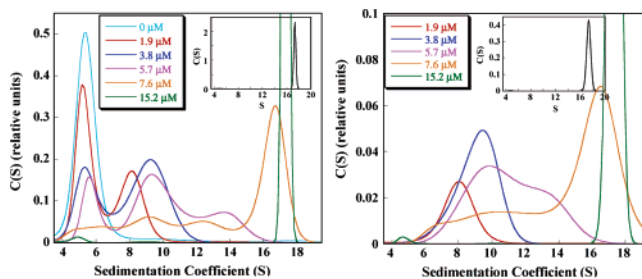


**Figure 3.** Sedimentation coefficient distribution *c*(*s*) derived from the sedimentation velocity data monitored at 262 nm (left) and 312 nm (right). The concentration of tubulin is 10  $\mu\text{M}$ , and the concentrations of **3** are 0, 1.9, 3.8, 5.7, 7.6, and 15.2  $\mu\text{M}$ . The ordinate is scaled for clarity of the *c*(*s*) distributions of the intermediates. The full scale *c*(*s*) distribution of the 15.2  $\mu\text{M}$  sample is shown in the inset.



**Figure 4.** Transmission electron micrograph of the tubulin ring induced by **3**.

dimer (dimer of  $\alpha/\beta$ -heterodimers) since it corresponds to the molar mass of 200 kDa when converted to the mass distribution. Moreover, 8.1 S is close to the predicted sedimentation coefficient (7.95 S) for tubulin dimer using the Kirkwood–Riseman approach.<sup>11</sup>

<sup>†</sup> Biophysics/Enzymology-Chemical and Screening Sciences.

<sup>‡</sup> Medicinal Chemistry-Chemical and Screening Sciences.

<sup>§</sup> Vaccines Research.

The presence of monomer and dimer at this ratio was confirmed using size-exclusion chromatography (SEC) coupled to multiangle laser light scattering (MALLS) to obtain the molar mass (data not shown). The ability to resolve monomer and dimer by SEC suggests that the rate of interconversion of the species is slow. It is interesting that the 5.3 S peak, corresponding to tubulin monomer, was not observed for the detection at 312 nm, the wavelength at which **3** absorbs. The inability to observe the inhibitor–tubulin monomer complex was also reported for dolastatin 10,<sup>12</sup> a tubulin inhibitor whose binding to tubulin is competitively inhibited by hemisterlin.<sup>1</sup> It is possible that **3** binds at the interface between two tubulin monomers. Alternatively, the inability to observe the ligand-bound tubulin monomer could be due to the reason that the concentration of tubulin used in this study is well above the dissociation constant of the liganded-tubulin dimer. The concentration of tubulin that can be used is limited by the necessity to maintain a low ratio of **3** to tubulin and at the same time allow the reliable absorbance measurement of **3**. To estimate the binding stoichiometry in the tubulin dimer, the overlapped peaks in the *c(s)* distribution at 262 nm were fitted to the Gaussian curves to resolve the individual peaks. Analysis of the area under each peak generates the protein concentration of 5.9  $\mu\text{M}$  for the 5.3 S species and 4.1  $\mu\text{M}$  for the 8.1 S species. The amount of inhibitor bound to the 8.1 S species was estimated from the area under the peak detected at 312 nm. This analysis yielded 1.9  $\mu\text{M}$  inhibitor and the binding stoichiometry of ca. 0.5, which corresponds to one inhibitor per tubulin dimer. The binding stoichiometry of 0.5 is consistent with the binding at the interface between two monomers. Alternatively, it could mean that the liganded-tubulin monomer can associate with either ligand-free or ligand-bound monomer to generate tubulin dimer.

When 3.8  $\mu\text{M}$  of **3** was added to 10  $\mu\text{M}$  tubulin, the resulting *c(s)* distributions show two peaks at 5.3 and 9.4 S detected at 262 nm but only one asymmetric peak at 9.4 S detected at 312 nm. The predicted sedimentation coefficient for tubulin trimer (trimer of  $\alpha/\beta$ -heterodimers) is 9.7 S in the linear arrangement and 10.6 S in the triangular arrangement. It is likely that the 9.4 S peak corresponds to tubulin trimer arranged in the linear fashion and the asymmetry comes from the presence of the small amount of dimer. Analysis of the area under the 9.4 S peak detected at 262 and 312 nm gives the binding stoichiometry of ca. 0.6, corresponding to approximately two inhibitors per tubulin trimer. The presence of monomer, dimer, and trimer at this ratio is also confirmed by the SEC/MALLS method.

At the ratios between 0.5 and 1, multiple intermediates exist. It is difficult to assign unambiguously the identity of each intermediate due to the peak overlap and possibly the small amount of it. These peaks are not analyzed further.

The distinct UV absorbance of **3** also allows us to probe its binding site. To verify that **3** binds tubulin at the same site as the parent inhibitor, HTI-286, different amounts of HTI-286 were added to the sample containing 10  $\mu\text{M}$  tubulin pre-incubated with 10  $\mu\text{M}$  of **3**. Sedimentation was monitored alternately at 262 and 312 nm. The amount of **3** bound to the ring structure of tubulin was estimated from the peak area in the *c(s)* distribution detected at 312 nm. With the addition of 10, 100, or 1000  $\mu\text{M}$  of HTI-286, the bound **3** was displaced by 27, 66, and 81%, respectively, suggesting that **3** binds tubulin at the same site as HTI-286 and the binding is reversible. We also compared the binding site of **3** with the classic antitubulin agent, colchicine. Colchicine has a distinct UV absorbance at 353 nm at which stilbene does not absorb (Figure 2). Colchicine alone does not induce tubulin oligomerization (Figure 5). However, in the sample containing equal amounts (10  $\mu\text{M}$ ) of **3**, colchicine, and

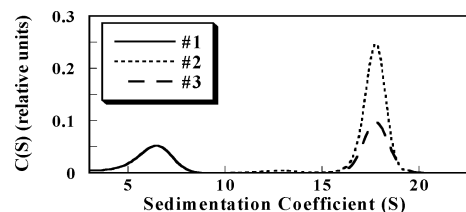


**Figure 5.** Sedimentation coefficient distribution *c(s)* derived from the sedimentation velocity data. Curve 1 is from the sample containing 10  $\mu\text{M}$  tubulin and 10  $\mu\text{M}$  colchicine, monitored at 353 nm; curves 2 and 3 are from the sample containing 10  $\mu\text{M}$  tubulin, 10  $\mu\text{M}$  **3**, and 10  $\mu\text{M}$  colchicine, monitored at 312 and 353 nm, respectively.

tubulin, the *c(s)* distribution shows a single peak at 17.4 S detected at 312 nm (signal dominated by **3**) and 353 nm (signal from colchicine alone) (Figure 5). This suggests that colchicine binds to the tubulin ring induced by the bound **3**. Peak area analysis indicated that equal amounts (10  $\mu\text{M}$ ) of **3** and colchicine bind the tubulin ring simultaneously. The structure of the ternary complex of tubulin with colchicine and the stathmin-like domain of RB3 was reported.<sup>13</sup> In the complex, colchicine binds  $\beta$ -subunit at the intradimer surface with  $\alpha$ -subunit. Consistent with these results, recent photoaffinity labeling studies at Wyeth<sup>5</sup> indicated that a photoaffinity analogue of HTI-286 cross-links to the  $\alpha$ -tubulin within the residues 314–339, which is distant from the colchicine binding site.

In summary, we obtained the binding stoichiometries in the intermediate oligomers and the final ring structure of tubulin during the ligand-induced association using the distinct absorbance of the stilbene analogue. This analogue also allows us to compare the binding site with other antitubulin agents.

**Supporting Information Available:** Synthesis procedures for the stilbene analogue and the spectral characterization. This material is available free of charge via the Internet at <http://pubs.acs.org>.

## References

- (1) Bai, R.; Durso, N. A.; Sackett, D. L.; Hamel, E. *Biochemistry* **1999**, *38*, 14302–14310.
- (2) Zask, A.; Birnberg, G.; Cheung, K.; Kaplan, J.; Niu, C.; Norton, E.; Suayan, R.; Yamashita, A.; Cole, D.; Tang, Z.; Krishnamurthy, G.; Williamson, R.; Khafizova, G.; Musto, S.; Hernandez, R.; Annable, T.; Yang, X.; Discafani, C.; Beyer, C.; Greenberger, L. M.; Loganzo, F.; Ayrál-Kaloustian, S. *J. Med. Chem.*, in press.
- (3) Loganzo, F.; Discafani, C. M.; Annable, T.; Beyer, C.; Musto, S.; Hari, M.; Tan, X.; Hardy, C.; Hernandez, R.; Baxter, M.; Singanallor, T.; Khafizova, G.; Poruchynsky, M. S.; Fojo, T.; Nieman, J. A.; Ayrál-Kaloustian, S.; Zask, A.; Andersen, R. J.; Greenberger, L. M. *Cancer Res.* **2003**, *63*, 1838–1845.
- (4) Krishnamurthy, G.; Cheng, W.; Lo, M.-C.; Aulabaugh, A.; Razinkov, V.; Ding, W.; Loganzo, F.; Zask, A.; Ellestad, G. *Biochemistry* **2003**, *42*, 13484–13495.
- (5) Nunes, M.; Kaplan, J.; Loganzo, F.; Zask, A.; Ayrál-Kaloustian, S.; Greenberger, L. M. *Eur. J. Cancer* **2002**, *38*, S119.
- (6) This stilbene analogue binds tubulin with slightly higher affinity compared to HTI-286 (apparent dissociation constant of 20 nM versus 100 nM) based on isothermal titration calorimetry (ITC) studies. The ITC experiments were conducted with the condition similar to that in ref 4 for the serial titration.
- (7) Frigon, R. P.; Timasheff, S. N. *Biochemistry* **1975**, *14*, 4559–4566.
- (8) Lobert, S.; Frankfurter, A.; Correia, J. J. *Biochemistry* **1995**, *34*, 8050–8060.
- (9) Barbier, P.; Gregoire, C.; Devred, F.; Sarrazin, M.; Peyrot, V. *Biochemistry* **2001**, *40*, 13510–13519.
- (10) Schuck, P. *Biophys. J.* **2000**, *78*, 1606–1619.
- (11) Bloomfield, V.; Dalton, W. O.; Van Holde, K. E. *Biopolymers* **1967**, *5*, 135–148.
- (12) Bai, R.; Taylor, G. F.; Schmidt, J. M.; Williams, M. D.; Kepler, J. A.; Pettit, G. R.; Hamel, E. *Mol. Pharmacol.* **1995**, *47*, 965–976.
- (13) Ravelli, R. B.; Gigant, B.; Curmi, P. A.; Jourdain, I.; Lachkar, S.; Sobel, A.; Knossow, M. *Nature* **2004**, *428*, 198–202.

JA048619E